



Time-resolved Measurements of Electric Field, Electron Temperature, and Electron Density in a Nanosecond-Pulsed Dielectric Barrier Discharge

Timothy Y. Chen¹, Benjamin M. Goldberg², Aric C. Rousso³, Yiguang Ju⁴, and Egemen Kolemen⁵
¹⁻⁵*Department of Mechanical and Aerospace Engineering, Princeton University, Princeton, NJ 08544*
²*Sandia National Laboratories, Livermore, CA 94550*

Abstract: Non-equilibrium low temperature plasmas are characterized by low neutral gas temperatures and highly energetic electrons that excite, ionize, and dissociate the neutral species. To understand the electron dynamics, the source of the electron energy, the electric field, and the electron properties, their temperature and density, must be measured in the same plasma. With these three parameters, a complete picture of the electron dynamics can be obtained. The electric field was measured using electric field induced second harmonic generation (E-FISH), while the electron temperature and density was measured through incoherent Thomson scattering. It was found that shortly after breakdown, a secondary discharge may have occurred to bring the electron density to measurable levels. Furthermore, the electrons did not decay below 0.5 eV even though the electric field was nearly zero, indicating superelastic collisions with Ar metastables could be important for heating the electrons.

1. Introduction

There is strong interest in utilizing non-equilibrium plasmas for plasma-assisted combustion [1], fuel reforming [2], and catalysis [3]. In these non-equilibrium discharges, highly energetic electrons are crucial in enabling and accelerating chemical reactions by exciting and dissociating reactants through electron-impact reactions. For example, in a plasma-assisted CH₄ oxidation study, Lefkowitz et al. found that most of the fuel consumption was either through dissociative electron-impact reactions or through reaction with O¹(D), an excited oxygen atom produced by electron-impact excitation [4]. The electron energy distribution (EEDF) and electron density govern the branching ratios of these electron-impact reactions and the subsequent chemistry. In addition, the electron energy originates from the electric field in the discharge gap which accelerates the electrons during breakdown. Unfortunately, in 0-D plasma chemistry models, E/N, the reduced electric field is pre-specified and treated as a fitting parameter [4,5]. As a result, there is uncertainty in the resulting chemical reaction pathways initiated by electron-impact. Therefore, time-resolved measurements of the electric field, electron temperature, and electron density would provide a complete profile of the discharge for understanding the non-equilibrium character of the discharge and for validating plasma chemistry models. However, many studies either measure the electric field or the electron density and temperature for model validation. For instance, Goldberg et al. measured the electric field in a nanosecond-pulsed dielectric barrier discharge (ns-DBD) with four-wave mixing and used the measured electric field to compute the electron density [6]. On the other hand, Roettgen et al. measured the electron temperature and density in a nanosecond-pulsed pin-to-pin discharge with Thomson scattering to validate a model that used the applied voltage [7]. Few combined time-resolved measurements of all three plasma properties exist in the literature for a volumetric nanosecond-pulsed discharge.

In this study, Thomson scattering and electric field-induced second harmonic generation (E-FISH) will be used to characterize the electron temperature, electron density, and electric field in a ns-DBD.

2. Experimental Methods

A modified version of the Thomson scattering setup in [8] was used in this study by adding a volume Bragg grating notch filter (Optigrate BNF-532-OD4-12.5M) to the collection optics. Thomson scattering is elastic scattering of light from electrons, and the resultant Doppler-broadened spectrum reflects the EEDF [9,10]. A 10 Hz frequency-doubled Quantel Q-Smart 850 Nd:YAG laser is focused to the center of the plasma reactor by an anti-reflection coated (AR coated) plano-convex lens (L1) with a focal length of 1.3 m. The reactor is made of quartz and has a gap distance of 14 mm with 44.5 mm square metal electrodes sandwiching the quartz on the outer surface. A 1-inch diameter AR

¹ Ph.D. Candidate, tc8@princeton.edu, Student Member AIAA.

² Postdoctoral Research Associate, Member AIAA

³ Ph.D. Candidate, Student Member AIAA.

⁴ Robert Porter Patterson Professor, Fellow AIAA.

⁵ Assistant Professor.

coated achromatic aspheric lens of focal length 60 mm (L2) collects the scattered light and focuses it into 7x1 linear fiber bundle with $200\mu\text{m}$ core diameter (Thorlabs BFA200HS02). A 75 mm focal length achromatic lens (L3) collimates the light and transmits it through the volume Bragg grating notch filter. After passing through the filter, a 100 mm focal length lens focuses the light from the fiber bundle into a f/6.5 spectrometer (Acton SpectraPro 2500i). Slit widths of 400 μm are used, and a 2400 grooves/mm holographic grating optimized for visible light disperses the light.

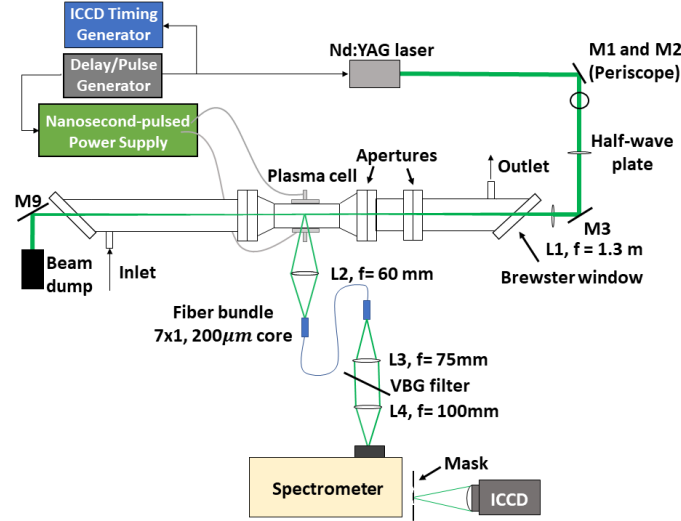


Figure 1. Experimental setup for the Thomson scattering measurement.

Thomson spectra are resolved by using a volume Bragg grating notch filter to attenuate light at 532 nm in conjunction with a blackened mask at the spectrometer focal plane. The notch filter first reduces the amount of stray light entering the spectrometer, and the mask physically blocks the Rayleigh scattering at 532 nm. This allows for high intensifier gain and long on-chip charge coupled device (CCD) accumulations without saturating the camera. A Princeton Instruments PIMAX 1300 intensified CCD (ICCD) camera with a UNIGEN II filmless intensifier is used to detect the signal photons. A delay generator (SRS DG645) is used to trigger the Nd:YAG laser, voltage power supply, and the ICCD. The laser pulse energy was measured before each measurement using a pyroelectric energy sensor (Ophir PE50BF-DIF-C) and was 350 mJ per pulse. Stray light, plasma emission, and dark current spectra are measured to subtract out any interfering signals. Absolute density calibration is done using Raman Scattering in N_2 at 75 Torr. Each Thomson spectrum is fit with a Gaussian profile to determine electron temperature, and the area under this Gaussian is integrated to infer the electron number density. A high voltage probe (Tektronix P6015A) was used to measure the voltage pulse and a photodiode was used to time the laser pulse with respect to the voltage pulse.

The electric field is measured using the E-FISH method which is a non-resonant *in-situ* laser diagnostic for the magnitude of the electric field [11–14]. In a symmetric and homogeneous medium, second harmonic generation is forbidden. However, once an electric field is applied, that symmetry is broken. This allows for the generation of coherent light by the neutral gases through a third order nonlinear optical process once a laser pulse is applied. The advantages of this technique include the coherent nature of the signal beam, the flexibility of gas mixtures that can be measured, and quadratic scaling of the signal with the magnitude of the electric field.

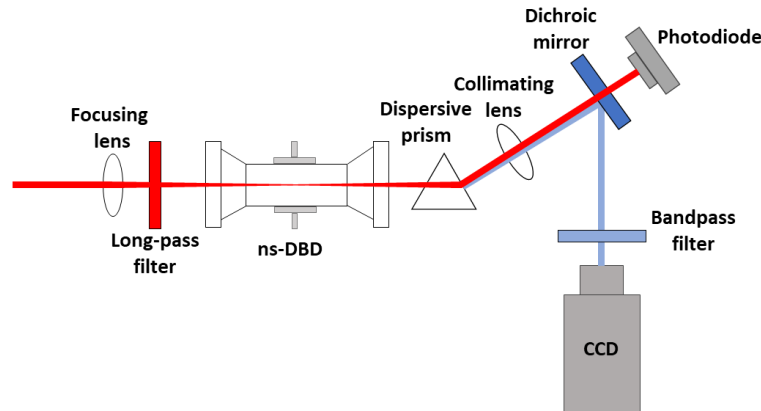


Figure 2. E-FISH experimental setup.

A schematic of the setup is shown in Figure 2. A Spectra-Physics Solstice Ace laser was used as the pump source and produces a 50 fs laser pulse centered at 800 nm with a 15 nm bandwidth. The laser was focused into a sheet at the center of the dielectric barrier discharge using an $f = 400$ mm cylindrical lens. The measurement length, which follows the laser confocal beam parameter, was ~ 2 cm, ensuring measurements were taken only within the diffuse plasma. Additionally, a laser sheet was used to minimize beam intensity while still allowing for significant signal generation due to the high intensity femtosecond laser source. This had the additional benefit of allowing for 1-D spatial sensitivity as a further diagnostic to verify the diffuse nature of the DBD plasma. After passing through the plasma region, the signal beam was collimated using a matched cylindrical lens and separated from the pump beam by a dispersive prism and a dichroic mirror. A PIXIS 512 CCD was used as the detector with a bandpass filter placed in front to limit interference from plasma emission. A 500 ms camera gate was used, effectively averaging 500 laser shots together. Additional averaging was achieved by collecting 10 images at each time step. Measurements were performed with 1 ns temporal resolution, as the laser jitter with respect to the discharge was measured to be less than 500 ps.

3. Results and Discussion

Thomson scattering and E-FISH measurements using pure Ar have been performed at 75 Torr. The voltage pulses were applied at a continuous 50 Hz repetition rate which was synchronized with the laser pulses using an SRS DG645 digital delay generator. From Figure 3, the electron temperature rapidly dropped from roughly 3 eV to 0.5 eV within the first 50 ns. Furthermore, the electron temperature did not continue decaying after reaching 0.5 eV. The electron number density grew above the detection limit of approximately $1 \times 10^{12} \text{ cm}^{-3}$ at 30 ns. Before 30 ns, a Thomson spectrum could not be resolved. Therefore, it is likely that the peak electron temperature was higher than 3 eV, but the electron density was too low to detect with the current setup. There was a local peak in the electron temperature at 30 ns, which is later shown in Figure 5 to be correlated with a rise in the electric field.

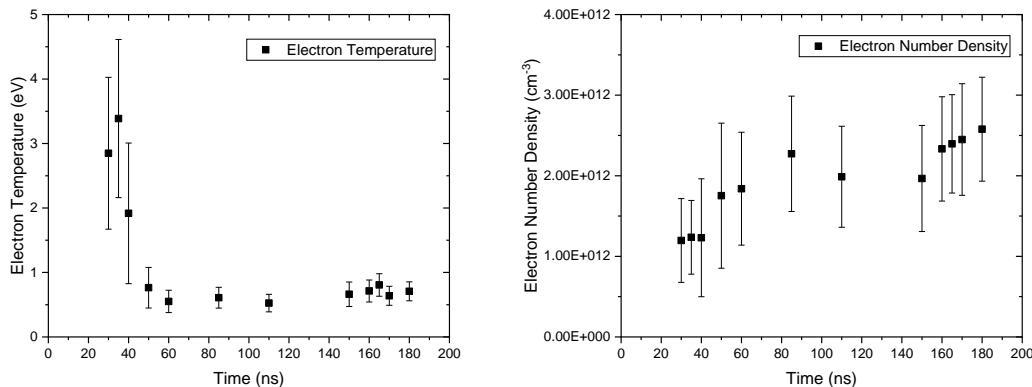


Figure 3. Electron density and temperature in an Ar ns-DBD as a function of time. The voltage pulse starts at $t = 0$.

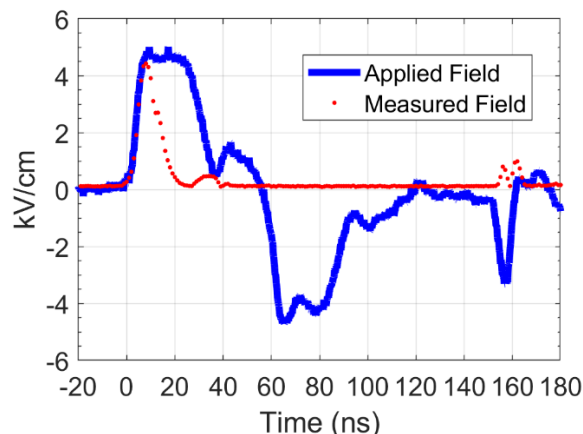


Figure 4. Electric field and applied field measurements as a function of time in an Ar ns-DBD.

Shown in Figure 4 is the time-resolved electric field measured by E-FISH and the applied field extrapolated from the measured voltage from a back current shunt in a pure Ar ns-DBD. The shown E-FISH signal is averaged across the cylindrically focused laser sheet.

The electric field closely followed the applied field until breakdown occurred. The sharp drop in electric field corresponds to establishment of a diffuse discharge. Following the initial drop, a smaller peak in electric field was observed near the end of the applied field pulse. The smaller peak indicates a response of the plasma to the decreasing applied field. A secondary reflected pulse appeared at 160 ns, with a small peak in the electric field at approximately 160 ns. The polarity of the applied field indicates a reversal in the electric field, but E-FISH is proportional to E^2 , so this cannot be directly confirmed.

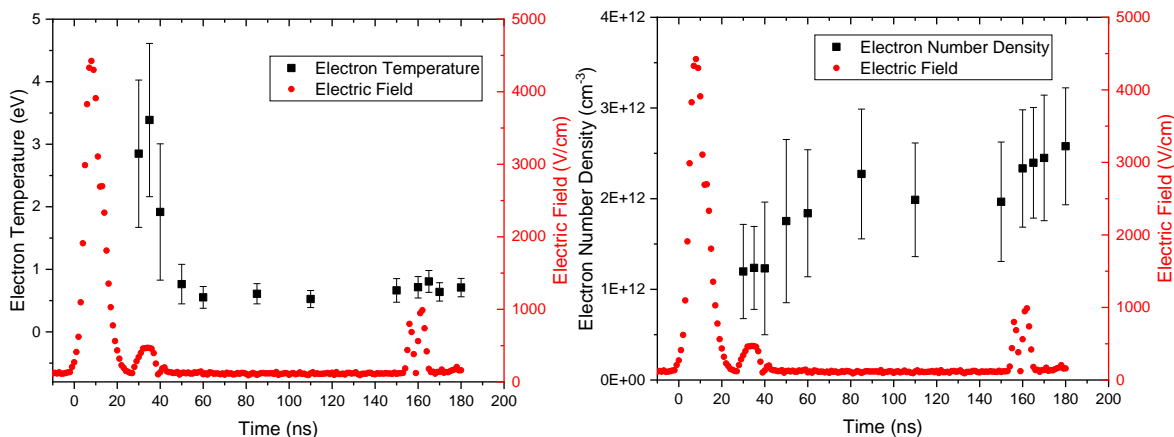


Figure 5. Electric field, electron temperature, and electron density as a function of time in an Ar ns-DBD.

Figure 5 shows Figures 3 and 4 plotted with each other. From Figure 5, several points of interest noted earlier can be explained. First, the observed electron heating is unlikely to have been from the electric field, as the electric field was nearly zero between 60 ns and 150 ns. This indicates that superelastic collisions with Ar metastables may play an important role in keeping the electrons heated above the neutral gas temperature, similar to the pure He discharge in [7]. Secondly, the small peak following the main pulse at 30 ns corresponds to the first detectable Thomson spectrum. This indicates that at this point, the plasma experiences a secondary discharge as a response to the applied field, thereby increasing the electron density to detectable levels. Finally, the two small peaks in the electric field appear to correspond with rises in the electron temperature. However, further measurements are required to confirm this point as the current signal-to-noise ratio is insufficient to make a definitive claim.

4. Conclusions

Thomson scattering and E-FISH measurements have been carried out in the same ns-DBD. The Thomson scattering measurements show that the electron temperature does not decay beyond 0.5 eV, indicating that superelastic collisions

may be important. The E-FISH measurement showed that during the falling edge of the main voltage pulse, a small peak in the electric field appeared, indicating a response from the plasma to the changes in the applied field. The E-FISH measurement also showed the existence of a secondary peak in the electric field from the reflected voltage pulse. From comparing both the E-FISH and Thomson scattering results, the electric field peak during the falling edge of the voltage pulse corresponded with the first detectable electron densities while the secondary peak in the electric field corresponded to a small rise in electron temperature and density. However, the uncertainty of the electron density and temperature measurements was larger than the evaluated rise for the secondary peak. In the future, a larger fiber bundle will be used to increase the amount of collected scattered light in the system and improve the signal-to-noise ratio to confirm these initial findings. These measurements will provide a greater understanding of the non-equilibrium electron dynamics in the ns-DBD and a more complete validation of plasma physics and chemistry models.

Acknowledgements

The authors would like to acknowledge the support from the U.S. Department of Energy, Office of Science, Office of Fusion Energy Sciences under award number DE-SC0020233, NSF grant CBET 1903362 and ExxonMobil through its membership in the Princeton E-filiates Partnership of the Andlinger Center for Energy and the Environment. TYC is partially supported through the Program in Plasma Science and Technology at Princeton University Fellowship.

References

- [1] Starikovskiy, A., and Aleksandrov, N. "Plasma-Assisted Ignition and Combustion." *Progress in Energy and Combustion Science*, Vol. 39, No. 1, 2013, pp. 61–110. doi:10.1016/j.pecs.2012.05.003.
- [2] Snoeckx, R., Aerts, R., Tu, X., and Bogaerts, A. "Plasma-Based Dry Reforming: A Computational Study Ranging from the Nanoseconds to Seconds Time Scale." *The Journal of Physical Chemistry C*, Vol. 117, No. 10, 2013, pp. 4957–4970. doi:10.1021/jp311912b.
- [3] Wang, L., Yi, Y., Wu, C., Guo, H., and Tu, X. "One-Step Reforming of CO₂ and CH₄ into High-Value Liquid Chemicals and Fuels at Room Temperature by Plasma-Driven Catalysis." *Angewandte Chemie International Edition*, Vol. 56, No. 44, 2017, pp. 13679–13683. doi:10.1002/anie.201707131.
- [4] Lefkowitz, J. K., Guo, P., Rousso, A., and Ju, Y. "Species and Temperature Measurements of Methane Oxidation in a Nanosecond Repetitively Pulsed Discharge." *Philosophical Transactions of the Royal Society A: Mathematical, Physical and Engineering Sciences*, Vol. 373, No. 2048, 2015, p. 20140333. doi:10.1098/rsta.2014.0333.
- [5] Rousso, A., Mao, X., Chen, Q., and Ju, Y. "Kinetic Studies and Mechanism Development of Plasma Assisted Pentane Combustion." *Proceedings of the Combustion Institute*, 2018. doi:10.1016/j.proci.2018.05.100.
- [6] Goldberg, B. M., Shkurenkov, I., O'Byrne, S., Adamovich, I. V., and Lempert, W. R. "Electric Field Measurements in a Dielectric Barrier Nanosecond Pulse Discharge with Sub-Nanosecond Time Resolution." *Plasma Sources Science and Technology*, Vol. 24, No. 3, 2015, p. 035010. doi:10.1088/0963-0252/24/3/035010.
- [7] Roettgen, A., Shkurenkov, I., Simeni Simeni, M., Petrishchev, V., Adamovich, I. V., and Lempert, W. R. "Time-Resolved Electron Density and Electron Temperature Measurements in Nanosecond Pulse Discharges in Helium." *Plasma Sources Science and Technology*, Vol. 25, No. 5, 2016, p. 055009. doi:10.1088/0963-0252/25/5/055009.
- [8] Chen, T. Y., Rousso, A. C., Wu, S., Goldberg, B. M., van der Meiden, H., Ju, Y., and Kolemen, E. "Time-Resolved Characterization of Plasma Properties in a CH₄/He Nanosecond-Pulsed Dielectric Barrier Discharge." *Journal of Physics D: Applied Physics*, Vol. 52, No. 18, 2019, p. 18LT02. doi:10.1088/1361-6463/ab0598.
- [9] Huang, M., Warner, K., Lehn, S., and Hieftje, G. M. "A Simple Approach to Deriving an Electron Energy Distribution from an Incoherent Thomson Scattering Spectrum." *Atomic Spectroscopy*, 2000, p. 14.
- [10] Sande, M. J. van de. *Laser Scattering on Low Temperature Plasmas: High Resolution and Stray Light Rejection*. Technische Universiteit Eindhoven, Eindhoven, The Netherlands, 2002.
- [11] Dogariu, A., Goldberg, B. M., O'Byrne, S., and Miles, R. B. "Species-Independent Femtosecond Localized Electric Field Measurement." *Physical Review Applied*, Vol. 7, No. 2, 2017. doi:10.1103/PhysRevApplied.7.024024.
- [12] Goldberg, B. M., Chng, T. L., Dogariu, A., and Miles, R. B. "Electric Field Measurements in a near Atmospheric Pressure Nanosecond Pulse Discharge with Picosecond Electric Field Induced Second Harmonic Generation." *Applied Physics Letters*, Vol. 112, No. 6, 2018, p. 064102. doi:10.1063/1.5019173.
- [13] Tang, Y., Simeni Simeni, M., Frederickson, K., Yao, Q., and Adamovich, I. V. "Counterflow Diffusion Flame Oscillations Induced by Ns Pulse Electric Discharge Waveforms." *Combustion and Flame*, Vol. 206, 2019, pp. 239–248. doi:10.1016/j.combustflame.2019.05.002.
- [14] Chng, T. L., Orel, I. S., Starikovskaia, S. M., and Adamovich, I. V. "Electric Field Induced Second Harmonic (E-FISH) Generation for Characterization of Fast Ionization Wave Discharges at Moderate and Low Pressures." *Plasma Sources Science and Technology*, Vol. 28, No. 4, 2019, p. 045004. doi:10.1088/1361-6595/ab0b22.